

Motion in the gravitational field of an oblate spheroid

Vladimir Ivchenko

*Department of Energy, Electrical Engineering and Physics,
Kherson National Technical University, Kherson 73008, Ukraine,
e-mail: reterty@gmail.com*

Received 19 December 2024; accepted 13 March 2025

We present the theory of motion in the gravitational field of an attracting object, considering its equatorial bulge. There is a secular precession of the orbit that occurs in the direction opposite to the orbital revolution. The precession rate increases as the gravitating body's flattening increases and the orbit's characteristic size decreases. Using the perturbation approach, we derive the equations for finding the precession period and the apocentric distance. We also construct the generalized version of the Laplace-Runge-Lenz vector for this type of motion.

Keywords: Equatorial bulge; secular precession; apocentric distance; perturbation approach; Laplace-Runge-Lenz vector.

DOI: <https://doi.org/10.31349/RevMexFisE.23.010208>

1. Introduction

There are countless objects in the universe that have an aspherical shape. Among them, you can often find bodies whose shape may be roughly approximated by an oblate spheroid (the ellipsoid of revolution or rotational ellipsoid). The reason for this is an equatorial bulge [1], which is described by a difference between the equatorial and polar diameters of an object due to the centrifugal force exerted by the rotation about the body's axis. Examples of such objects are: planet Saturn (eccentricity $\varepsilon = 0.432$; Fig. 1), star Archenar with $\varepsilon = 0.66$, dwarf elliptical galaxy M32 with $\varepsilon = 0.49$, etc.

It is well known that the field strength of any uniform body of spherical shape is inversely proportional to the square of the distance between the sphere center and the observation point as in the case of the point mass model. Our experience shows that many students leave introductory physics courses with the impression that in the calculation of gravitational force, the entire mass of any extended object can always be assumed to be located at its center of mass. At the same time, some other students (puzzling the author), repeatedly asked how the deviations from the spherical shape should modify the usual Keplerian orbits of the satellites.

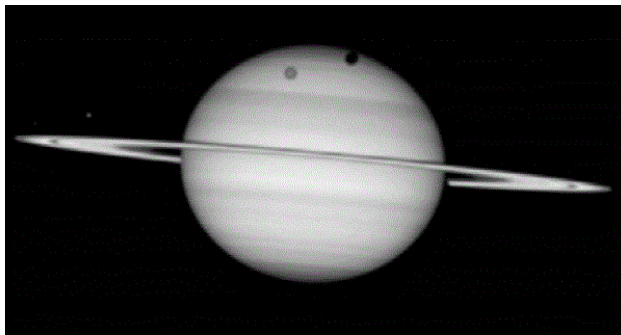


FIGURE 1. The planet Saturn is approximately in the shape of an oblate spheroid with eccentricity $\varepsilon = 0.432$.

The first effect caused by the equatorial bulge is nodal precession [1]. Nodal precession is the precession of the orbital plane of a satellite around the rotational axis of an astronomical body such as Earth. Renzetti [2, 3] has studied the influence of different types of non-sphericity of gravitating bodies on satellite orbital precessions.

Another important effect is an axial precession. This is a gravity-induced, slow, and continuous change in the orientation of an astronomical body's rotational axis. As Newton pointed out in his "Principia", the oblateness of the Earth along the axis of rotation leads to the fact that the gravitational attraction of the bodies of the solar system causes the precession of the Earth's axis. In Newton's mathematical model, the Earth was mentally divided into a spherical part and a ring-shaped equatorial thickening. From the laws of mechanics discovered by Newton, it followed that the attraction of the Moon (and to a lesser extent the Sun) creates an additional torque for the thickening, leading to a rotation of the Earth's axis.

In this paper, we give a detailed analysis of the satellite's orbital motion (apsidal precession) in the presence of a slightly oblate spheroidal object. This issue is an accessible and instructive topic for undergraduates studying an advanced course in classical mechanics. Moreover, it helps readers identify how deviations from the point mass model affect the orbital motion patterns of satellites.

2. Theory

The multipole expansion for the gravitational potential energy of a spheroid, including only the first two terms, has the following form [4]:

$$U(r) \approx -\frac{GMm}{r} + GQ_{zz}m \frac{3\cos^2\theta - 1}{4r^3}, \quad (1)$$

where G is the gravitational constant, M is the mass of a gravitating object, m is the mass of a satellite, Q_{zz} is the gravitational quadrupole moment. Equation (1) is written in

the spherical coordinate system, where r is the radial distance, and θ is the polar angle. The quadrupole moment can be expressed via the components of the moment of inertia tensor. For an oblate spheroid [4]:

$$Q_{zz} = 2(I_{xx} - I_{zz}) = -\frac{2Ma^2\varepsilon^2}{5}, \quad (2)$$

where a is the equatorial radius of an oblate spheroidal object. Therefore, the value of Q_{zz} is negative for an oblate spheroid (for a prolate spheroid, Q_{zz} is positive).

Using the relation $\mathbf{F} = -\nabla U$ and Eq. (1), we get:

$$\mathbf{F} = Gm \left[\left(-\frac{M}{r^2} + \frac{3Q_{zz}(3\cos^2\theta - 1)}{4r^4} \right) \hat{\mathbf{e}}_r + \frac{3Q_{zz}\sin 2\theta}{4r^4} \hat{\mathbf{e}}_\theta \right], \quad (3)$$

where $\hat{\mathbf{e}}_r$ and $\hat{\mathbf{e}}_\theta$ are the spherical unit vectors. Thus, in the general case, \mathbf{F} is a non-central force. However, for the orbits in the equatorial plane ($\theta = \pi/2$), \mathbf{F} is still a central force even in the presence of a non-zero value of Q_{zz} . In what follows, we shall consider only these stable orbits (this property directly follows from Eq. (3)). In the case $\theta = \pi/2$, the angular momentum \mathbf{L} is still a conserved quantity even if $Q_{zz} \neq 0$. Moreover, employing Bertrand's theorem [5], we can state a priori that in our case, all bound orbits are not closed orbits.

Now, we introduce the focal parameter of the conical section:

$$p = \frac{L^2}{GMm^2} = \text{const}, \quad (4)$$

where L is the absolute value of the angular momentum \mathbf{L} . Denoting $u = p/r = 1/\rho$ (ρ is the dimensionless radial distance), and using the approach of Ref. [6], we get at the following differential equation given the shape of the orbital motion (the Binet equation):

$$\frac{d^2u}{d\varphi^2} + u = 1 - \alpha u^2, \quad (5)$$

where φ is the azimuthal angle and

$$\alpha = \frac{3|Q_{zz}|}{4Mp^2} = \frac{3}{10} \left(\frac{a\varepsilon}{p} \right)^2 > 0, \quad (6)$$

is the parameter of our problem ($\alpha \ll 1$). Equation (5) is known as the equation of the quadratic non-linear oscillator. Let us proceed to the new variables:

$$v = \frac{\alpha}{\sqrt{1+4\alpha}} \left(u - \frac{\sqrt{1+4\alpha}-1}{2\alpha} \right), \quad (7)$$

$$\phi = (1+4\alpha)^{1/4} \varphi.$$

Then Eq. (5) takes the simplest possible form:

$$\frac{d^2v}{d\phi^2} + v + v^2 = 0. \quad (8)$$

Equation (8) is a second-order differential equation requiring two initial conditions for a unique solution. We choose the periapsis (the point of closest approach of a satellite to spheroid) as the starting point. At this point the radial component of the velocity (dr/dt) turns to zero. But,

$$\frac{du}{d\varphi} = -\frac{p}{r^2} \frac{dr}{dt} \frac{1}{d\varphi/dt},$$

where $d\varphi/dt \neq 0$ is the angular speed. Therefore, our initial conditions are as follows:

$$u(0) = 1 + e, \quad \left. \frac{du}{d\varphi} \right|_{\varphi=0} = 0, \quad (9)$$

where e is the eccentricity of a conic section (the orbit) at $\alpha = 0$. In this case

$$v(0) = \frac{\alpha}{\sqrt{1+4\alpha}} \left(1 + e - \frac{\sqrt{1+4\alpha}-1}{2\alpha} \right) = A, \quad (10)$$

$$\left. \frac{dv}{d\phi} \right|_{\phi=0} = 0.$$

The exact solution to equations (8), and (10) has the following form [7]:

$$v(\phi) = A - 6m\omega^2 \text{sn}^2(\omega\phi, m), \quad (11)$$

where $\text{sn}(z, m)$ is the Jacobian elliptic sine function of real argument z [8];

$$\omega = \sqrt{\frac{1+2A}{4(1+m)}}, \quad (12)$$

$$m = \frac{1}{2} + \frac{3(2A^2 + 2A - 1)}{3 + (1+2A)\sqrt{3(1-2A)(3+2A)}}, \quad (13)$$

is the square modulus of the function sn .

At $\alpha = 0$, we have: $m = 0$, $\omega = 1/2$ and $u(\varphi) = 1 + e \cos \varphi$. This is the case of ordinary Keplerian orbits (ellipses, parabolas, or hyperbolas, depending on the value of parameter e). At $\alpha \neq 0$, there is a secular (apsidal) precession of the orbit that occurs in the direction opposite to the orbital revolution (Fig. 2).

Moreover, the shape and size of the satellite's orbit undergo some variations (Fig. 3). In particular, the apocentric distance somewhat increases.

3. The perturbation approach

To describe quantitatively both effects found in a simple way (in terms of parameter $\alpha \ll 1$), we apply the perturbation technique based on the method of variation of constants [9]. We write the solution of unperturbed ($\alpha = 0$) Eq. (5) in the form:

$$u_0(\varphi) = 1 + e \cos(\varphi - \varphi_0), \quad (14)$$

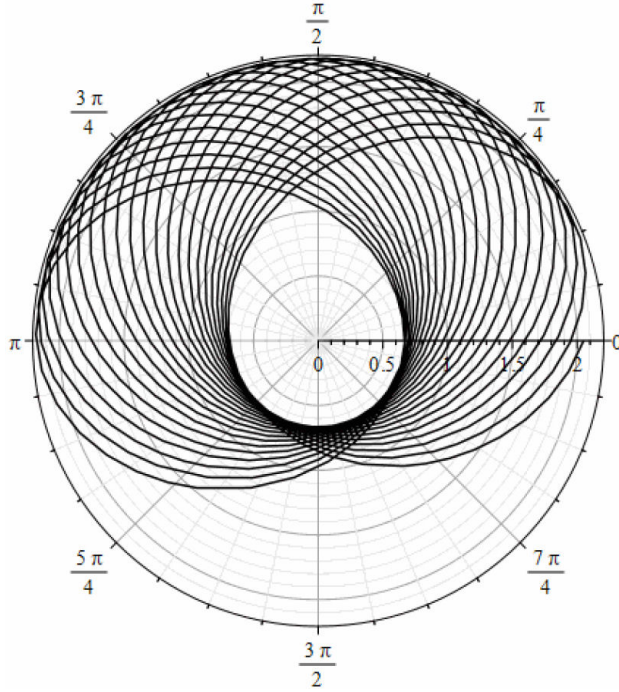


FIGURE 2. The polar plot $\rho(\varphi)$ (Rosetta orbit) according to Eq. (10). $\alpha = 0.02$, $e = 0.5$.

where we can set, for simplicity, the initial angle φ_0 equal to zero. Now, we search for the solution of perturbed Eq. (5) in form (16), considering the integration constants e and φ_0 now depend on the variable φ , that is

$$u(\varphi) = 1 + e(\varphi) \cos(\varphi - \varphi_0(\varphi)). \quad (15)$$

Straightforward calculations lead to the following differential system in e and φ_0 :

$$\begin{cases} \cos \varphi \frac{de}{d\varphi} + e \sin \varphi \frac{d\varphi_0}{d\varphi} = 0 \\ -\sin \varphi \frac{de}{d\varphi} + e \cos \varphi \frac{d\varphi_0}{d\varphi} = -\alpha(1 + e \cos \varphi)^2 \end{cases}. \quad (16)$$

The solution to this system is:

$$\varphi_0(\varphi) = -\frac{\alpha}{e} \left[e\varphi + \sin \varphi \left(1 + \frac{2e^2}{3} + e \cos \varphi + \frac{e^2 \cos^2 \varphi}{3} \right) \right], \quad (17)$$

$$e(\varphi) = e + \frac{\alpha}{3e} [(1+e)^3 - (1+e \cos \varphi)^3]. \quad (18)$$

The change of φ_0 over an entire revolution period is:

$$\Delta \varphi_0 = \varphi_0(2\pi) - \varphi_0(0) = -2\pi\alpha. \quad (19)$$

Therefore, for each revolution of the body along the quasi-ellipse, the perihelion shifts in the direction opposite to the direction of revolution by an angle equal to $2\pi\alpha$. In this case, the precession period (in fractions of the orbital period T_0) is given by:

$$\frac{T_p}{T_0} = \frac{1}{\alpha}. \quad (20)$$

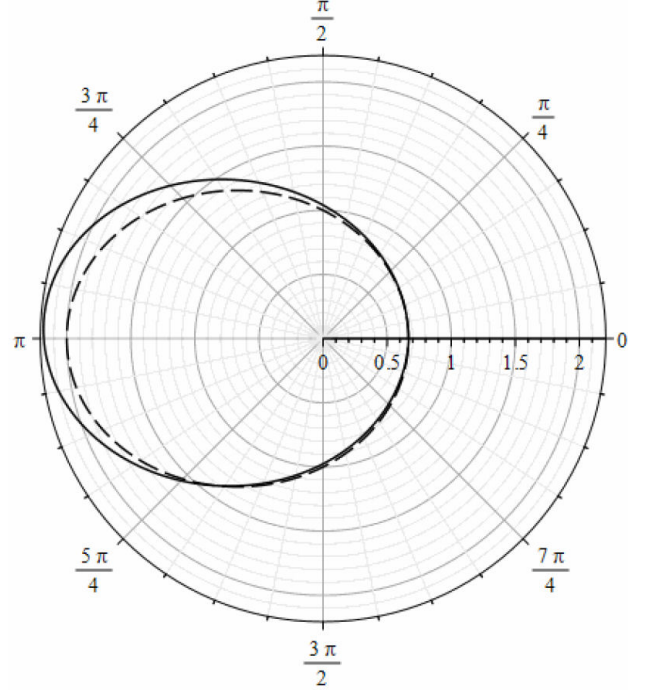


FIGURE 3. The satellite's orbits at $e = 0.5$. Dashed line: $\alpha = 0$ (ellipse); solid line: $\alpha = 0.02$.

Equations (20) and (6) tell us that the precession rate increases with an increase in the degree of flattening of the gravitating body and a decrease in the characteristic size of the orbit. It is precisely this circumstance that explains the fact that the orbit of Saturn's innermost ring D68 is characterized by significant precession [10] (the same behavior is observed for the orbits of Saturn's inner moons).

The apocentric distance r_a for the quasi-elliptical orbit can be found as:

$$\begin{aligned} \frac{r_a}{r_0} &= \frac{1-e}{u(\pi)} \\ &= \frac{1-e}{1 - \left(e + \frac{\alpha}{3e} [(1+e)^3 - (1-e)^3] \right) \cos(\pi\alpha)}, \end{aligned} \quad (21)$$

where r_0 is the apocentric distance for the unperturbed ($\alpha = 0$) case. As e increases, the difference between r_a and r_0 increases too (Fig. 4). At some critical value $e_{cr} < 1$ the distance r_a becomes infinitely large, and for $e > e_{cr}$ the orbits are open (quasi-hyperbolas). As the parameter α increases, the value of e_{cr} decreases.

4. The generalized Laplace-Runge-Lenz vector

In Kepler's problem, in addition to the total energy and angular momentum, the conserved quantity is also the Laplace-Runge-Lenz (LRL) vector. The LRL vector is defined as [5]

$$\mathcal{A} = \mathbf{p} \times \mathbf{L} - GMm^2 \hat{\mathbf{e}}_r, \quad (22)$$

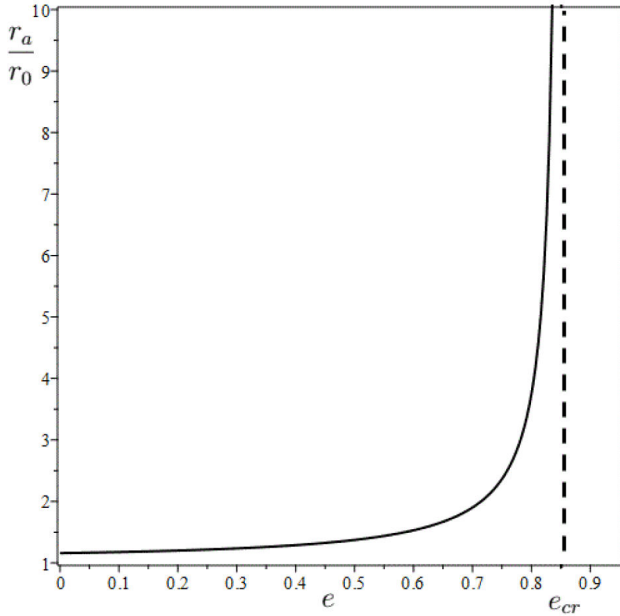


FIGURE 4. Dependence $r_a(e)$ at $\alpha = 0.07$.

where \mathbf{p} is the momentum of a moving body. Thus, this quantity can be represented as the difference between two vectors, one of which is the vector product of another two vectors. According to Eq. (22), the LRL vector always lies in the plane of the orbit and parallel to the apsidal line. In the limiting case of a circular orbit, the LRL vector is equal to zero.

The conservation of the LRL vector is intimately linked with the fact that the orbit closes. The advantage of using the LRL vector is that it allows one to bypass the need for direct integration of the equations of motion, immediately providing information about the geometry of the orbit [5].

In the presence of the second term in Eq. (1), the LRL vector is no longer a conserved quantity. Instead, we can write “the equation of motion of \mathcal{A} ”. For the case $F_r \propto 1/r^4$, this equation reads as [5]

$$\dot{\mathcal{A}} = -\frac{3G|Q_{zz}|m^2}{4r^2}\dot{\mathbf{e}}_r, \quad (23)$$

(here we use dot notation for time derivative). Since

$$\dot{\mathbf{e}}_r = \dot{\varphi} \hat{\mathbf{e}}_\varphi = \dot{\varphi} (-\sin \varphi \hat{\mathbf{e}}_x + \cos \varphi \hat{\mathbf{e}}_y), \quad (24)$$

and $dt = mr^2 d\varphi / L$, Eq. (23) takes form:

$$\frac{d\mathcal{A}}{d\varphi} = -\alpha GMm^2 u^2(\varphi) (-\sin \varphi \hat{\mathbf{e}}_x + \cos \varphi \hat{\mathbf{e}}_y). \quad (25)$$

In the first order of perturbation theory, we can put $\alpha u(\varphi) \approx \alpha u_0(\varphi)$ (see Eq. (14)) and solve Eq. (25). Then

$$\mathcal{A}^* = \mathcal{A} + \alpha GMm^2 \left[\frac{u_0^3(\varphi)}{3e} \hat{\mathbf{e}}_x + \left(e\varphi + \frac{\sin \varphi (e^2 \cos^2 \varphi + 3e \cos \varphi + 2e^2 + 3)}{3} \right) \hat{\mathbf{e}}_y \right]. \quad (26)$$

be the generalized LRL vector, which is a conserved quantity for our type of motion. The importance of Eq. (26) is that it tells us that in the presence of the equatorial bulge, the orientation of the apsidal line changes over time [due to the presence of the azimuthal angle in Eq. (26)].

5. Conclusion

In this paper, we demonstrate that deviations from the model of the gravitational field of a point mass cause both changes in the shape and size of the satellite’s orbit and its secular precession. This analysis highlights the limitations of the point-source field model, offering readers insight into its applicability.

Additionally, we derive and solve the equation of a quadratic non-linear oscillator, a topic of significant educational value. The concept of non-linearity is a cornerstone of modern physics, carrying profound scientific importance. Next, we introduce the reader to elements of perturbation theory, a powerful tool widely utilized in contemporary celestial mechanics. Finally, we construct the generalized version of the Laplace-Runge-Lenz vector, which is a conserved quantity for our type of motion.

1. F. D. Stacey and P. M. Davis, *Physics of the Earth* (4th edition, Cambridge University Press, UK, 2008). <https://doi.org/10.1017/CBO9780511812910>
2. G. Renzetti, Satellite Orbital Precessions Caused by the Octupolar Mass Moment of a Non-Spherical Body Arbitrarily Oriented in Space, *J. Astrophys. Astron.* **34** (2013) 341, <https://doi.org/10.1007/s12036-013-9186-4>
3. G. Renzetti, Satellite orbital precessions caused by the first odd zonal J3 multipole of a non-spherical body arbitrarily oriented in space, *Astrophys. Space Sci.* **352** (2014) 493, <https://doi.org/10.1007/s10509-014-1915-x>
4. V. Ivchenko, What is the most “non-point” gravitating or electrically charged object?, *Rev. Mex. Fis. E* **17** (2020) 69, <https://doi.org/10.31349/RevMexFisE.17.69>
5. H. Goldstein, C. P. Poole and J. L. Safko, *Classical Mechanics* (3rd edition, Pearson Education, Inc., publishing as Addison-Wesley, 2002).
6. N. Samboy and J. Gallant, A modern interpretation of Newton’s theorem of revolving orbits, *Am. J. Phys.* **92** (2024) 343, <https://doi.org/10.1119/5.0166698>
7. H. Hu, Exact solution of a quadratic nonlinear oscillator, *J. Sound Vib.* **295** (2006) 450, <https://doi.org/10.1016/j.jsv.2006.01.013>
8. M. Abramowitz and I. A. Stegun, *Handbook of Mathematical Functions with Formulas, Graphs, and Mathematical Tables* (1st edition, Washington D.C.; New York, Dover Publications, 1983), Ch. 16.

9. L. Barbieri and F. Talamucci, *Calculation of Apsidal Precession via Perturbation Theory*, *Adv. Astrophys.* **4** (2019) 96, <https://dx.doi.org/10.22606/adap.2019.43003>
10. M. M. Hedman, J. A. Burt, J. A. Burns and M. R. Showalter, *Non-circular features in Saturn's D ring: D68, Icarus* **233** (2014) 147, <https://doi.org/10.1016/j.icarus.2014.01.022>